Ecotoxicology and Environmental Safety 286 (2024) 117110

Contents lists available at ScienceDirect

Ecotoxicology and Environmental Safety

journal homepage: www.elsevier.com/locate/ecoenv

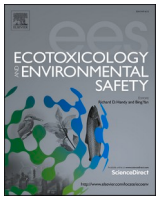

A Copula-based spatiotemporal probabilistic model for heavy metal pollution incidents in drinking water sources

Jing Liu [a,1], Xiaojuan Xu [a,1], Yushun Qi [b], Naifeng Lin [a], Jinwei Bian [c], Saige Wang [d,e,*], Kun Zhang [a], Yingying Zhu [a], Renzhi Liu [b], Changxin Zou [a,**]

[a] Nanjing Institute of Environmental Sciences, Ministry of Ecology and Environment of the People's Republic of China, Nanjing 210042, China
[b] State Key Laboratory of Water Environment Simulation, School of Environment, Beijing Normal University, No. 19, Xinjiekouwai Street, Haidian District, Beijing 100875, China
[c] School of Resources and Environment, Hunan University of Technology and Business, Changsha 410205, China
[d] School of Energy and Environmental Engineering, University of Science & Technology Beijing, Beijing 100083, China
[e] Advancing Systems Analysis (ASA) Program International Institute for Applied Systems Analysis, Laxenburg 2361, Austria

ARTICLE INFO

Edited by Dr. HAO ZHU

Keywords:
Accidental heavy metal pollution
Drinking water source
Copula analysis
Spatiotemporal probabilistic distribution
Yangtze River

ABSTRACT

Water pollution incidents pose a significant threat to the safety of drinking water supplies and directly impact the quality of life of the residents when multiple pollutants contaminate drinking water sources. The majority of drinking water sources in China are derived from rivers and lakes that are often significantly impacted by water pollution incidents. To tackle the internal mechanisms between water quality and quantity, in this study, a Copula-based spatiotemporal probabilistic model for drinking water sources at the watershed scale is proposed. A spatiotemporal distribution simulation model was constructed to predict the spatiotemporal variations for water discharge and pollution to each drinking water source. This method was then applied to the joint probabilistic assessment for the entire Yangtze River downstream watershed in Nanjing City. The results demonstrated a significant negative correlation between water discharge and pollutant concentration following a water emergency. The water quantity-quality joint probability distribution reached the highest value (0.8523) after 14 hours of exposure during the flood season, much higher than it was (0.4460) during the dry season. As for the Yangtze River downstream watershed, five key risk sources (N1–N5) and two high-exposure drinking water sources (W3–W4; AEI=1) should be paid more attention. Overall, this research highlights a comprehensive mode between water quantity and quality for drinking water sources to cope with accidental water pollution.

1. Introduction

Water pollution accidents, are considerably unpredictable, have high toxicity and enduring consequences, pose severe threats to water safety and the overall health of aquatic ecosystems. Ultimately, such incidents can disrupt social and economic stability (Issakhov et al., 2021; Liu et al., 2024). When these contaminants infiltrate drinking water sources, they pose an immense danger to the safety of the drinking water supply, and directly affect public health and livelihoods (Liu et al., 2021a; Manyepa et al., 2024). Drinking water sources in China primarily originate from rivers or lakes (Zhai et al., 2021) that are vulnerable to unforeseen events (Wang et al., 2023). The frequency of emergencies that affect drinking water source protection areas has notably elevated (Xu et al., 2021; Meng et al., 2024). Upon the occurrence of accidents, spatiotemporal variations in water discharge are strongly disturbed, resulting in water quality fluctuation, that exacerbate the difficulty of accurately simulating pollutant concentration variations in real time compared with a typical water environment. Therefore, the accurate characterization of the internal mechanism linking water discharge and pollutant concentration in aquatic environments (Paredes-Arquiola et al., 2010; Liu et al., 2018; Wang et al., 2024) during accidental water pollution remains a crucial challenge.

Due to the bioaccumulation, poisonousness, and non-biodegradation of heavy metals (Ali et al., 2022), there are inadvertent adverse effects

* Corresponding author at: School of Resources and Environment, Hunan University of Technology and Business, Changsha 410205, China.
** Corresponding author.
E-mail addresses: saige@ustb.edu.cn (S. Wang), zcx@nies.org (C. Zou).
[1] These authors contributed equally

https://doi.org/10.1016/j.ecoenv.2024.117110
Received 29 April 2024; Received in revised form 29 July 2024; Accepted 24 September 2024
Available online 15 October 2024
0147-6513/© 2024 Published by Elsevier Inc. This is an open access article under the CC BY-NC-ND license (http://creativecommons.org/licenses/by-nc-nd/4.0/).

on the proper functioning of groundwater systems that pose significant health risks (Dippong et al., 2022). Pollution indices, such as the heavy metal pollution index (Dippong and Resz, 2024 a), cluster analysis (Varol and Tokatli, 2023), and multivariate statistical approaches (Varol and Tokatli, 2022), have been used to assess heavy metal contamination in water bodies. These mathematical models primarily rely on extensive temporal and spatial datasets of water samples, that incorporate specific parameters and standard values. Subsequently, these data undergo a transformation process that assigns scores to classify fluids into separate categories that accurately represent the specific degree of contamination (Dippong and Resz, 2022). However, heavy metal ions (i.e., water quality) would inevitably be impacted by discharge (i.e., water quantity) in a waterbody. Therefore, it is imperative to study the relationship between these two variables.

Water quantity (i.e., discharge) and quality (i.e., pollutant concentration) are the two essential characteristics of waterbodies. A meticulous understanding of their underlying mechanisms is fundamental for the effective management of aquatic environments (Campanho et al., 2021; Li et al., 2023). Typically, these two variables have a significant negative correlation, suggesting that optimizing water quality via rational water scheduling represents a primary approach for water pollution mitigation strategies (Shokri et al., 2014; Yu et al., 2016; Zhao et al., 2024). For several decades, numerical models and multi-objective index methods have been the predominant approaches to investigate integrated assessments of water discharge and pollutant concentrations (Liu et al., 2022; Dippong et al., 2023). Numerical simulation depends on mature hydrological models, such as the Quality Model (QUAL; Hur et al., 2018; Shi et al., 2024), Water Quality Analysis Simulation Program (WASP; Mbuh et al., 2019; Huang et al., 2024), Distributed hydrodynamic and water quality model (HydroPol2D; Gomes et al., 2023), MIKE 21 model (Yang et al., 2021), Soil and Water Assessment Tool (SWAT; Xue et al., 2021; Shin et al., 2023) and so on, that provide frameworks for the analysis of complex water systems to predict the outcomes of various environmental scenarios. While these models excel at accurately forecasting the spatial and temporal dynamics of water quality, they fall short in elucidating the intricate interplay between water quantity and quality. This limitation stems from their narrow focus on the spatiotemporal distribution of specific contaminants, rather than considering the broader systemic interactions that govern water quality (Yu and Zhang, 2021; Liu et al., 2022). Multi-objective index methods encompass a variety of techniques, such as the composite index (He et al., 2023; Zavareh et al., 2023), the fuzzy index (Wang et al., 2014; Manzar et al., 2022), machine learning (Jiang et al., 2021; Najafzadeh et al., 2024), and linear additivity (Cao et al., 2021). It is important to acknowledge that while sophisticated models integrate a diverse array of natural, hydrological, and anthropogenic factors, these studies treat water discharge and pollutant concentration as isolated elements without accounting for their potential interactions.

As a powerful probabilistic technique for investigating relationships of random variables (Cai et al., 2023; Li et al., 2023), Copula functions (Sklar, 1959) enable the construction of multivariate joint probability distributions, facilitating a precise quantification of the dependency structures among these variables (Frees and Valdez, 1998). Copula functions allow for the creation of a joint probability distribution model that accurately captures any underlying nonlinear or asymmetric relationships between variables, ensuring that the model remains undistorted (Zentner, 2017; Cai et al., 2019). With fewer data parameters (McManamay, 2014), the Copula model is more flexible and has been widely applied in water environment management, including water resource allocations (Chen et al., 2022; Yue et al., 2022), water–energy nexus (Cai et al., 2019; Zhang et al., 2023) and water pollution assessments (Zang et al., 2022; Seo et al., 2024). Increased research attention has been directed toward understanding the relationship between water quantity–quality (Wang et al., 2017; Park et al., 2019) and water quality–quality for contaminants such as NH_3–N and COD_{Mn} (Liu et al., 2018, 2022), Polycyclic Aromatic Hydrocarbons (PAHs; Liu et al., 2020), and water quality forecasting (Zhang et al., 2024) in rivers or reservoirs under steady states. While several studies have investigated accidental heavy metal joint pollution, such as Cr^{6+}–Hg^{2+} (Liu et al., 2021b), there is a notable lack of research that has examined the internal relationships between water quality and quantity during periods of instability. Therefore, Copula techniques also have the potential to provide flexible simulations and accurate estimations of joint probability distributions for these two variables and can decrease bias in exposure assessments.

To fill this knowledge gap, in this study, a Copula-based probabilistic model is proposed to explore the internal mechanism between water quantity (i.e., discharge) and quality (i.e., pollutant concentration) during emergency water pollution incidents that affect drinking water sources. The innovations are as follows: (1) Copula functions are first introduced to explore the internal correlation between quantity and quality during water pollution emergencies, and then to estimate their joint probability distributions for each risk source across varying water sources. This provides a comprehensive understanding of the combined impact on water quality. (2) By integrating the sudden heavy metal transport model with hydrological simulations, it is possible to determine the real-time water discharge and pollutant concentration of drinking water sources across baseline and accident scenarios during the dry/flood season. (3) A kernel density analysis was preferentially adopted to fit the marginal probability of these two variables (i.e., water quantity and quality) within each unique scenario for different water sources. This model was applied to the Yangtze River downstream watershed in Nanjing, China, to identify the key risk sources, quantify the joint relationships between water quantity and quality, and ultimately clarify the spatiotemporal exposure distribution map of each drinking water source. This is essential for preventing risk sources, optimizing water dispatching strategies, and safeguarding sensitive ecological receptors to ensure the protection of drinking water sources.

2. Methods and materials

2.1. Study area and data sources

2.1.1. Study area

The Yangtze River has a length of 6380 km and a drainage area of 1.8×10^6 km^2 and is the longest river in China. It originates east of the Qinghai Tibetan Plateau and then flows into the East China Sea (Müller et al., 2008; Dong et al., 2023). The Yangtze River not only is the home of more than 4300 species of aquatic life but also contains approximately 400 million people, spanning 19 provinces from Western China to Eastern China (Chen et al., 2020). Its downstream (27′02″–35′08″N, 114′54″–123′10″E, see Fig. 1(a)) reaches extend from Hukou to the sea and include the Anhui, Jiangsu, Zhejiang Provinces and Shanghai City, with an area of 359,100 km^2 (He et al., 2023). This study focused on the Yangtze River downstream in Nanjing City of Jiangsu Province (see Fig. 1(b)). The Yangtze River is the most important drinking sources of Nanjing City and comprises seven designated intakes: three on the left bank (labeled W1, W2, and W4) and four on the right bank (labeled W3, W5–W7). These sources collectively provide water for an estimated population of 8.5 million residents in the city. As a golden waterway, the Yangtze River has fostered the growth of extensive water-based transport networks and numerous industrial operations along its banks. However, this development has also led to increased vulnerability to sudden pollution incidents, posing a significant environmental risk. Numerous industrial parks are situated within 5 km along the downstream of the Yangtze River that may pose a threat to drinking water sources. In our study, we selected 29 electroplating enterprises (labeled N1–N29) as representative risk sources for simulating accidental water

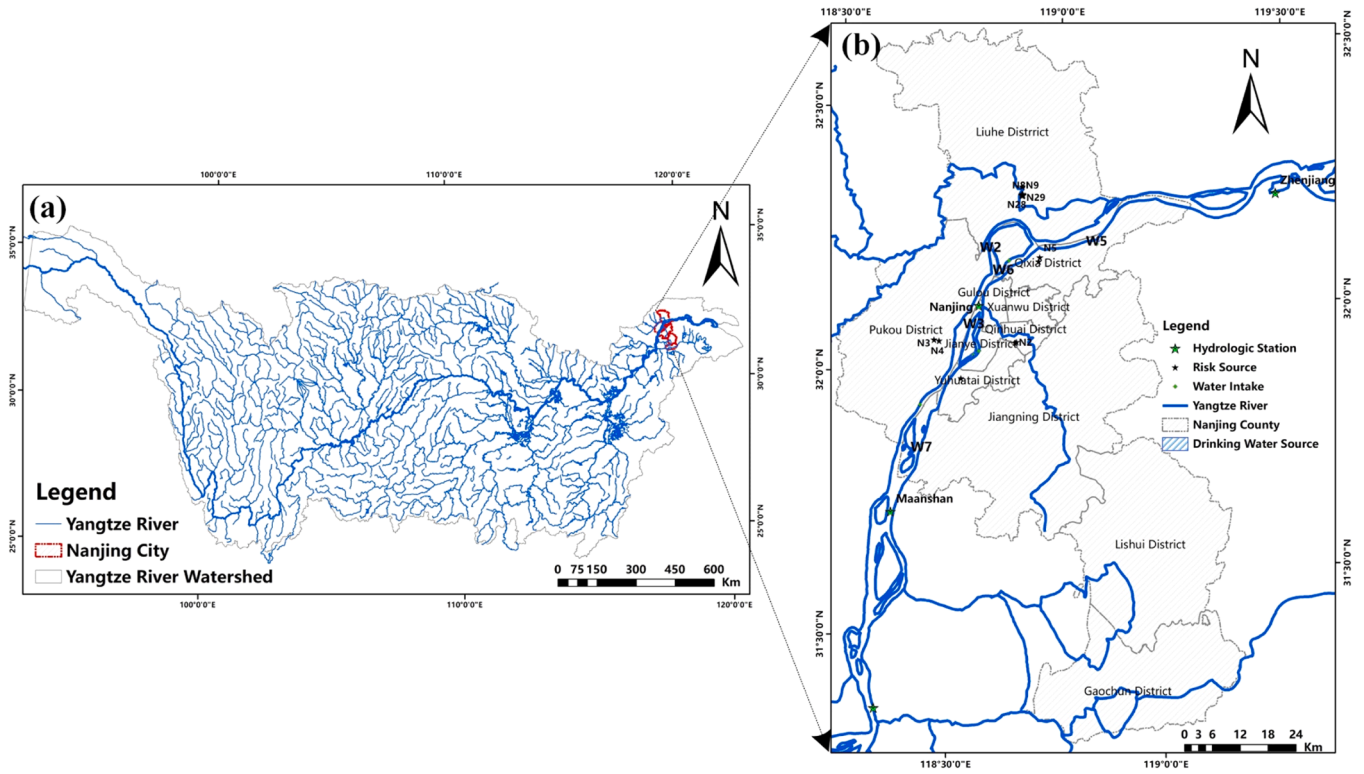

Fig. 1. Yangtze River (a) and its downstream watershed in Nanjing City (b).

pollution scenarios in the lower reach of the Yangtze River based on a checklist of typical heavy-metal enterprises in Nanjing City.

2.1.2. *Data sources and parameter establishments*

For each identified risk source, we meticulously gathered critical information such as its geographic coordinates, yearly wastewater discharge figures, peak concentrations of heavy metal ions, contingency plans for spill responses, associated costs, and details of the receiving water bodies. These data were sourced from their respective environmental risk management plans and detailed reports. In addition, field investigations were conducted in March 2023, in partnership with the Nanjing Eco-environment Bureau. As for the drinking water source, its spatial location, and daily water supply and intake, water intake location, and division of protection areas were obtained from the Jiangsu Province Water Resources Bulletin (Jiangsu, 2021) and local investigation reports on the basic situation of centralized drinking water source areas. Topographic data for the lower Yangtze River downstream of Nanjing were derived from a 30 m resolution Digital Elevation Model (DEM) sourced from the China Center for Resources Satellite Data and Application (CRESDA). We utilized digitally rendered topography data of the river, extracted from the 1:40,000 scale electronic navigational channel chart created by the Nanjing Navigation Bureau in 2009. Daily tide data (i.e., two high tide levels and two low tide levels) from the Ma'anshan Station, the Nanjing Station, and the Zhenjiang (II) Stations were selected from the annual hydrological report of the Yangtze River Basin (Ministry of Water Resources, 2019). The baseline concentrations of heavy metals in the sediment and surface water of the Yangtze River's lower reach were sourced from published studies (Zhang et al., 2017; Jin et al., 2023).

For the Yangtze River downstream watershed, we collected data on the boundary tide level and discharge from two stations (Ma'anshan and Zhenjiang (II)) during two time periods, i.e., the dry season (from 00:00 on February 1, 2018, to 00:00 on May 1, 2018) and the flood season (from 00:00 on June 1, 2018–00:00 on September 1, 2018). The calibration data were derived from the Nanjing Station. Regarding the accidental heavy metal pollution situation, the information was based on the prioritized list of heavy metal ions that require control in the lower reach of the Yangtze River, as well as the list of key enterprises responsible for monitoring heavy metal levels in 2018. The simulation parameters were determined using data from previous water pollution incidents in the Yangtze River downstream watershed (Wang et al., 2023; Xie et al., 2023), as well as insights gained from previous studies on heavy metal pollution (Liu et al., 2021a, 2021b). In this research, it was assumed that wastewater would be directly exposed to the Yangtze River water body once the emergency incident occurred.

Based on the list of priority control pollutants in the lower Yangtze River downstream of Nanjing City and the list of key monitoring and basic emission information of heavy metal enterprises in Jiangsu Province in 2018, four heavy metals (i.e., Cr^{6+}, Hg^{2+}, Pb^{2+}, and Cd^{2+}) were selected as the typical priority pollutants. According to the maximum credit accident theory (Khan, 2001), the maximum concentration of acute Cr^{6+} exposure was selected to simulate for each enterprise based on the Environmental Statistics for Nanjing City of Jiangsu Province in 2018. The onset of leakage occurred precisely at 00:00 on the 11th of February during the dry season simulation and the 11th of June during the flood season simulation. The leakage persisted for two hours.

2.2. *Model framework*

A Copula-based spatiotemporal probabilistic model (Fig. 2) was proposed to accurately forecast the interdependencies between water quantity, as measured by discharge, and water quality, characterized by pollutant concentrations, within drinking water source environments. This is, to our knowledge, the first systematic attempt to probabilistically predict the joint causal connections between water discharge and acute heavy metal ion exposure following an emergency that transpired at the watershed scale. This method comprised three main steps. First, a simulation model was developed to predict the temporal and spatial changes in water quantity and quality in the event of an accidental heavy metal emergency at the downstream watershed of the Yangtze

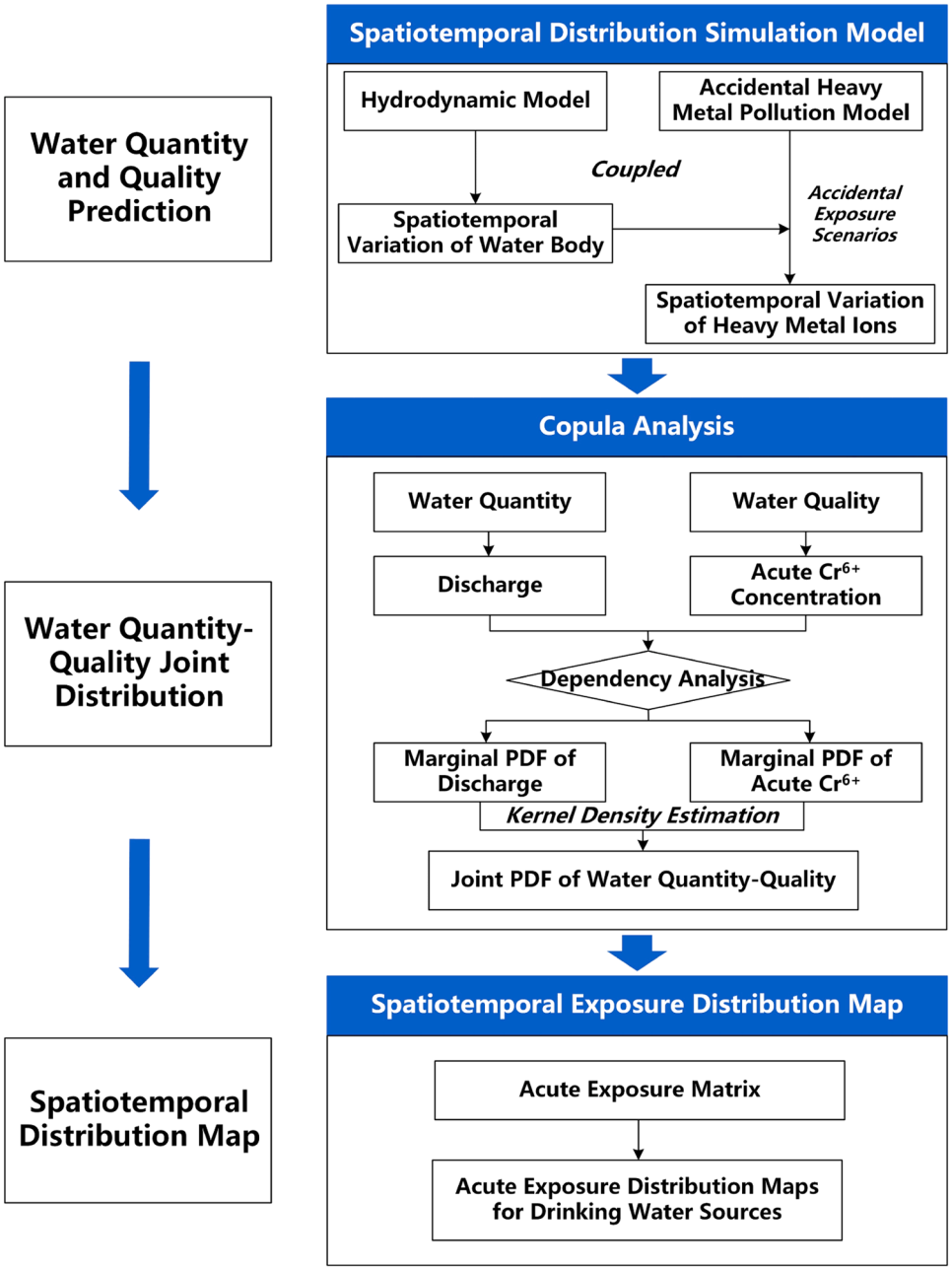

Fig. 2. Copula-based spatiotemporal probabilistic model framework.

River in Nanjing City. Second, marginal probability distributions of the water discharge and heavy metal ions were calculated based on a Kernel density analysis. Third, the joint probability distribution of these two variables was determined using a Copula analysis for each drinking water source in Nanjing City along the Yangtze River. Finally, a spatiotemporal distribution map of the entire watershed was constructed based on the acute exposure matrix of each identified risk source.

2.3. Spatiotemporal distribution simulation model

A spatiotemporal distribution simulation model was constructed to predict the time variation in water discharge and heavy metal concentration in the Nanjing section of the Yangtze River in response to potential accidental heavy metal pollution events. This integrated model comprised two components: a hydrological model for simulating varying river flows, discharge, and water levels, and a sudden heavy metal transport model for predicting the dispersion and fate of heavy metals in the event of contamination (Warren and Bach, 1992; Liao et al., 2020). Moreover, the sudden heavy metal transport model, proposed by Di Toro et al. (1986), was utilized to trace the spatiotemporal distribution of the dissolved and adsorbed heavy metal ions between the water and sediment phases.

Hydrological model: As the width of the Yangtze River in Nanjing City is much greater than its depth, and there is no obvious layering phenomenon, a two-dimensional hydrodynamic model was chosen to simulate the water levels and flows using MIKE 21 software, as shown in Eqs. 1–3. The water level variations were described by integrating the conservation of mass and momentum equations over the vertical, based on the Navier–Stokes equation with three incompressible and uniformly distributed Reynolds values (DHI, 2017a).

$$\frac{\partial Q}{\partial t}+\frac{\partial \Psi}{\partial x}+\frac{\partial \Omega}{\partial y}=S \tag{1}$$

$$Q = \begin{bmatrix} H \\ Q_x \\ Q_y \end{bmatrix}, \Psi = \begin{bmatrix} Q_x \\ UQ_x + gH^2/2 \\ UQ_y \end{bmatrix} \Omega = \begin{bmatrix} Q_y \\ UQ_x \\ UQ_y + gH^2/2 \end{bmatrix} \quad (2)$$

$$S = \begin{bmatrix} i \\ -\frac{gH\partial z_B}{\partial x} - C_f U\sqrt{U^2+V^2} \\ -\frac{gH\partial z_B}{\partial y} - C_f V\sqrt{U^2+V^2} \end{bmatrix} \quad (3)$$

where x, y and t represent the horizontal coordinate, vertical coordinate, and time, respectively; the vector Q consists of the water depth and the flow rates Q_x and Q_y; the variables U and V denote the velocity of flow in the x and y directions, respectively; the variables Ψ and Ω stand for the flux vectors in the x and y directions, respectively; the source term, vector S, consists of three components i.e., the rainfall of the infiltration term i, the bottom slope source term, and the frictional force term; z_B represents of the elevation of the riverbed bottom; and C_f is the roughness of the riverbed, $C_f = gn^2/h^{1/3}$, where n stands for the Manning coefficient.

The MIKE 21 HD flow model uses an Alternating Direction Implicit (ADI) method to numerically integrate the equations that govern the conservation of mass and momentum across both space and time dimensions, thereby providing a robust framework for simulating fluid dynamics. A Double Sweep (DS) was used to perform the resolution of the equation matrices that were produced for each individual grid line and each direction independently.

Sudden heavy metal transport model: Heavy metals in an aquatic environment can either be dissolved in water or attached to suspended particulate matter (Nyjfeler et al., 1986; Liu et al., 2021b). The behavior of heavy metal ions in aquatic environments typically includes the following processes Honeyman and Santschi, (1988): metal adsorption and desorption; particulate metal sedimentation and resuspension; dissolved metal diffusive transport at the sediment/water interface; and dissolved and particulate metal's advection and dispersion in the water column, as shown in the Eqs. 4–9.

$$\frac{dS_{HM}}{dt} = -\text{ adsorption} + \text{desorption} + \text{diffusion}\left[\frac{gMe}{m^3 bulk \cdot d}\right] \quad (4)$$

$$\frac{dS_{HMS}}{dt} = -\text{ adsorption} + \text{desorption} - \text{diffusion}\left[\frac{gMe}{m^2 \cdot d}\right] \quad (5)$$

$$\frac{dX_{HM}}{dt} = \text{adsorption} - \text{desorption} - \text{sedimentation} + \text{resuspension}\left[\frac{gMe}{m^3 bulk \cdot d}\right] \quad (6)$$

$$\frac{dX_{ss}}{dt} = \text{production} - \text{sedimentation} + \text{resuspension}\left[\frac{gDW}{m^3 bulk \cdot d}\right] \quad (7)$$

$$\frac{dX_{HMS}}{dt} = \text{adsorption} - \text{desorption} + \text{sedimentation} - \text{resuspension}\left[\frac{gMe}{m^2 \cdot d}\right] \quad (8)$$

$$\frac{dX_{SED}}{dt} = \text{sedimentation} - \text{resuspension}\left[\frac{gDW}{m^2 \cdot d}\right] \quad (9)$$

where S_{HM} and X_{HM} are the concentrations of heavy metals that have been dissolved and adsorbed in the water; S_{HMS} and X_{HMS} are the concentrations of heavy metals that have been dissolved and adsorbed in the sediment; X_{HMS} is the concentration of heavy metals that attached to sediment; and X_{SS} is the concentration of suspended solids in the water. More detailed equations can be found in the reference (DHI, 2017b).

2.4. Copula-based joint probability analysis

2.4.1. Dependence of water quantity and quality

The Spearman (ρ_n), Pearson (r_n), and Kendall (τ_n) correlation coefficients (Cai et al., 2019; Liu et al., 2021b) were calculated to clarify the relevance between random variables (i.e., water discharge and heavy metal ion concentration in short term), shown in Eqs. 10–12.

$$\rho_n = \frac{\sum_{i=1}^{n}(R_i - \overline{R})(S_i - \overline{S})}{\sqrt{\sum_{i=1}^{n}(R_i - \overline{R})^2 (S_i - \overline{S})^2}} = \frac{12}{n(n+1)(n-1)}\sum_{i=1}^{n} R_i S_i - \frac{3(n+1)}{n-1} \quad (10)$$

$$r_n = \sum_{i=1}^{n}(X_i - \overline{X})(Y_i - \overline{Y}) \Big/ ((n-1)\sqrt{S_x{}^2 S_y{}^2} \quad (11)$$

$$\tau_n = \frac{2}{n(n-1)}\sum_{i=1}^{n-1}\sum_{j=i+1}^{n} \text{sgn}((X_i - X_j)(Y_i - Y_j)) \quad (12)$$

where $\overline{X}$, $\overline{Y}$, $\overline{R}$, and $\overline{S}$ are the average values of X_i, Y_i, R_i and S_i, respectively; $S_x{}^2$ and $S_y{}^2$ are the variance values of X_i and Y_i, respectively; S_i is the order of Y_i in the sequence of $Y_1, Y_2, \ldots, Y_n$; R_i is the order of X_i in the sequence of $X_1, X_2, \ldots, X_n$; n is the sample length; sgn = −1 when $(X_i - X_j)(Y_i - Y_j) > 0$; sgn = 0 when $(X_i - X_j)(Y_i - Y_j) = 0$; and sgn = 1 when $(X_i - X_j)(Y_i - Y_j) < 0$.

2.4.2. Marginal probabilistic distributions establishment

The probability density functions (PDF) for water discharge and contaminant pollution were subsequently estimated using kernel density analysis (KDA) that provides a non-parametric way to estimate the underlying density of a random variable. A KDA aims to generate innovative samples from the original dataset's components, carefully crafted to mirror the original distribution's dispersion and key attributes, including its standard deviation, mean, and other statistical measures. The KDA, as defined by Tai and Uhlen (2015); Schleich and Wartzack (2018); and Goka et al. (2019), can be described as follows:

The sequence $A_1, A_2, \ldots A_n$ is selected from a continuous set of a single-dimensional examples whose KDE of the general density function, F(a), for any given point can be expressed using the Eq. 13.

$$\widehat{F(a)} = \frac{1}{nh}\sum_{i=1}^{n} K\left(\frac{A_i - a}{h}\right) \quad (13)$$

where the kernel function is denoted as $K(\cdot)$, and the bandwidth is characterized as h. The kernel estimation function utilizes the Gaussian kernel function. Therefore, the Gaussian kernel was selected for this research, as shown in the Eq. 14.

$$K(\widehat{u}) = \frac{1}{\sqrt{2\pi}}\exp\left(-\frac{1}{2}\widehat{u}^2\right) \quad (14)$$

where $\widehat{u} = (x - X_i)/h$.

2.4.3. Joint probability distribution constructions

The internal mechanism between water quantity (discharge) and quality (contaminant pollution) was explored using the effective Copula functions after constructing the marginal probability density function (PDF). Copula functions allow for the connection of various marginal distributions, resulting in the derivation of the corresponding joint probabilistic distribution functions; as proposed by (Sklar, 1959). The Copula model, known for its flexibility and variability, has been widely utilized in finance and is also extensively applied within the fields of water resources and energy. The fundamental principle of the Copula function (Eq. 15) is that it serves to link the marginal distributions with the overall joint distribution.

$$F(\alpha_1, \alpha_2, \ldots\ldots, \alpha_n) = C(F_{A_1}(\alpha_1), F_{A_2}(\alpha_2), \ldots\ldots, F_{A_n}(\alpha_n)) \quad (15)$$

where $F(\alpha_1, \alpha_2, \ldots\ldots, \alpha_n)$ is the joint distribution function; and $F_{A_1}(\alpha_1)$, $F_{A_2}(\alpha_2), \ldots\ldots, F_{A_n}(\alpha_n)$ are the marginal distribution functions of random variables $A_1, A_2, \ldots\ldots, A_n$. In this study, we selected the Copula functions (Eq. 16) with one parameter, such as the binary Normal Copula, Gumbel, Clayton and Frank Copulas, to facilitate generation (Cai et al., 2019; Zang et al., 2022). The fundamental structures of the Copula functions were introduced in the following manner, while the distinct variations of each Copula function are displayed in Table 1.

$$C(M, N, \theta) = \Phi_\theta(\Phi^{-1}(M), \Phi^{-1}(N)) \tag{16}$$

where θ presents the Copula function parameter; and $C(X, Y)$ stands for the binary Copula functions of the parameter of the Copula function to M and N, i.e., $M = F_{X_1}(\alpha_1)$, $N = F_{X_2}(\alpha_2)$.

In addition, the square Euclidean distance (Eq. 17) was introduced to test the fitting degree (Cai et al., 2019). The smaller the value of D^2, the better the fitting effect.

$$D^2 = \sum_{i=1}^{n} |C(M, N) - C_0(M, N)|^2 \quad , \tag{17}$$

where $C_0(M, N) = \frac{1}{n}\sum_{i=1}^{n} I[F_n(M_i \le M) I[F_n(N_i \le N]\,], \quad M, N \in [0, 1]$ is the empirical Copula function.

2.5. Spatiotemporal distribution map at the watershed level

Following the prediction of joint probabilities for an individual risk source, the overlaying exposure influence for each drinking water source was quantitatively computed using an acute exposure index (AEI, Table 2). The natural interval classification method was used to assign natural breaks to the exposure distribution for every drinking water source as follows: 0–0.25 (Zero), 0.25–0.5 (Low), 0.5–0.75 (Medium), and 0.75–1 (High). Subsequently, a spatiotemporal distribution map was created using ArcGIS technology to achieve a spatial representation and comparative analysis of the risks.

3. Results

3.1. Spatiotemporal distribution simulation under different scenarios

A spatiotemporal distribution simulation was first conducted for each risk source (N1–N29) under both baseline and accident situations. The Pujiang electronic electroplating plant (N3) was selected as the typical case to exhibit the spatiotemporal distribution. As the Cr^{6+} ions in the leakage wastewater of N3 exceeded water quality criteria, this was chosen as the typical heavy metal for the simulation process. Under the accident scenario, we assumed the leakage concentration of the Cr^{6+} ion was 60 mg/L, with a daily discharge (0.7075 m^3/s), extending over a duration of two hours. Therefore, the heavy metal emergency was set to occur at 00:00 on February 11th during the dry season simulation and on June 11th during the flood season simulation, separately. Measurement data from the Nanjing Station were selected to verify the spatiotemporal distribution model, as shown in Fig. 3. R^2 indicates that the hydrodynamic model fits the observed data well during both the dry (R^2=0.9274) and flood (R^2=0.9749) seasons. Therefore, the model can be used to simulate water flow, water level, and discharge for the Yangtze River downstream watershed.

Table 2
Acute exposure index distribution.

Acute Exposure Index		Flood season	
		Zero	Exposure
Dry Season	Zero	0	0.5
	Exposure	0.5	1

Once accidents happen, the heavy metal pollution would influence drinking water sources W4, W6, W1, W2, and W5, in sequence. Fig. 4 shows the spatiotemporal distribution of water discharge and acute Cr^{6+} pollution during the dry (February to March, 2018) and flood (July to September, 2018) seasons under the baseline and accident scenarios. For the variable of water quantity, discharges exhibited fluctuating states for each drinking water source during both the dry and flood seasons (see Table 3). The average value of Q during the flood season was approximately twice as high as during the dry season. For the water quality variable, the average Cr^{6+} concentration was 1.75 times higher during the flood season than during the dry season under the baseline scenario. Under the accident scenario, exceedances in the standard process lasted four hours during the dry season while three hours in flood season at drinking water source W4. In addition, the highest concentration of acute Cr^{6+} pollution occurred at 0.018765 mg/L at W4 at 17:30 on February 11th, 2018, during the flood season. Furthermore, the maximum concentration of acute Cr^{6+} pollution was 0.01695524 mg/L at W4 at 14:00 on June 11th, 2018, and 0.011 mg/L at W2 at 23:00 on June 11th, 2018, during the dry season.

3.2. Joint probability distribution of a single risk source

After the spatiotemporal dynamic simulation, the hourly water discharge and Cr^{6+} concentration distributions in each drinking water source were obtained during the dry and flood seasons for risk sources (N1–N29). Based on the kernel density analysis, the marginal probability distributions were then constructed, and the accident scenario of

Table 1
Copula functions and the Copula probability density functions.

Binary Copula		Functions
Normal	Copula	$C(M,N;\theta) = \int_{-}^{\varphi^{-1}(M)}\int_{-}^{\varphi^{-1}(N)} \frac{1}{2\pi\sqrt{1-\theta^2}} \exp\left[\frac{-(s^2+t^2-2\theta st)}{2(1-\theta^2)}\right] dsdt\ ,\ (\theta \in [-1,1])$
	PDF	$c(M,N;\theta) = \frac{1}{\sqrt{1-\theta^2}} \exp(-\frac{\varphi^{-1}(M)^2+\varphi^{-1}(N)^2-2\alpha\varphi^{-1}(M)\varphi^{-1}(N)}{2(1-\theta^2)}) \exp(-\frac{\varphi^{-1}(M)^2\varphi^{-1}(N)^2}{2})$
Frank	Copula	$C(M,N;\theta) = -\frac{1}{\theta}\ln\left[1+\frac{(e^{-\theta M}-1)(e^{-\theta N}-1)}{e^{-\theta}-1}\right],\ (\theta \neq 0)$
	PDF	$c(M,N;\theta) = \frac{-\theta(e^{-\theta}-1)e^{-\theta(M+N)}}{[(e^{-\theta}-1)+(e^{-\theta M}-1)(e^{-\theta N}-1)]^2}$
Clayton	Copula	$C(M,N;\theta) = (M^{-\theta}+N^{-\theta}-1)^{-\frac{1}{\theta}},\ (\theta > 0)$
	PDF	$c(M,N;\theta) = (1+\theta)(MN)^{-\theta-1}(M^{-\theta}+N^{-\theta}-1)^{-2-\frac{1}{\theta}}$
Gumbel	Copula	$C(M,N;\theta) = \exp\left\{-\left[(-\ln M)^\theta + (-\ln N)^\theta\right]^{\frac{1}{\theta}}\right\},\ (\theta > 1)$
	PDF	$c(M,N;\theta) = \frac{C(M,N,\theta)(\ln M \times \ln N)^{\theta-1}}{MN[(-\ln M)^\theta + (-\ln N)^\theta]^{2-\frac{1}{\theta}}}\left\{\left[(-\ln M)^\theta + (-\ln N)^\theta\right]^{\frac{1}{\theta}} + \frac{1}{\theta} - 1\right\}$

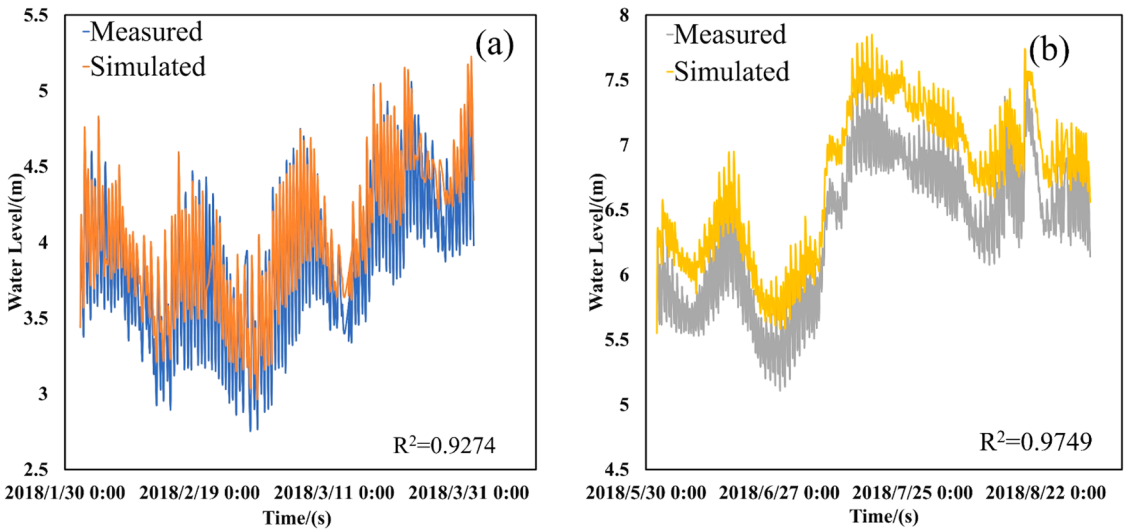

Fig. 3. Hydro-dynamic variation at the Nanjing hydrologic stations during the dry and flood seasons: measured VS simulated curves.

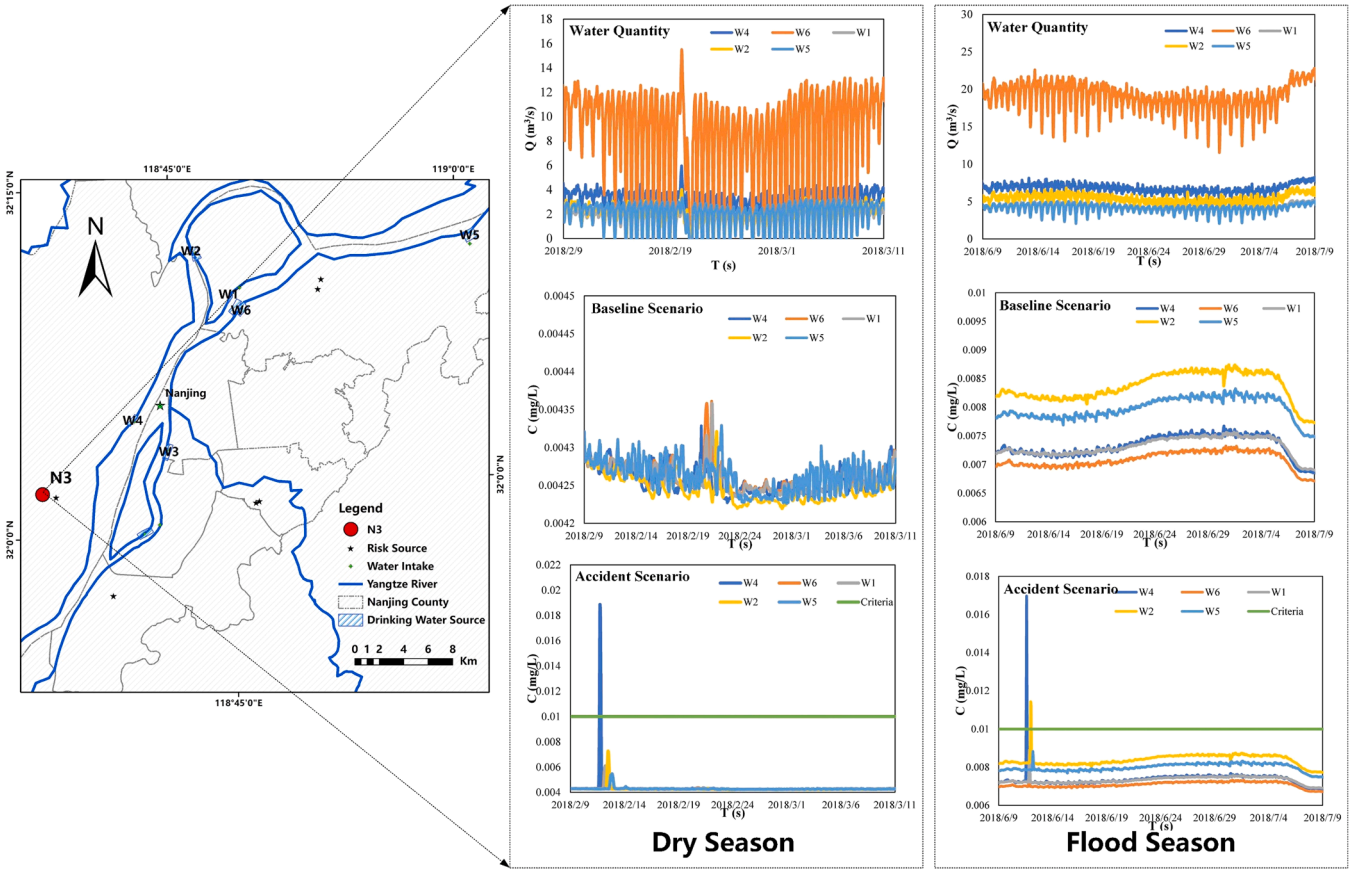

Fig. 4. Water quality and quantity after accidents in the different water sources.

N3 is shown in Fig. 5. Table 3 shows the marginal probabilities associated with acute exposure to Cr^{6+} ions that exceeded the thresholds established under the accident scenario. For comparison, the corresponding marginal probabilities under the baseline scenario, captured at the same time points, are also included in the table. Regarding water discharge, it was evident that the marginal probability distributions were identical under both the baseline and accident scenarios. In general, there was a gradual decrease in water flow within four hours of acute exposure during the dry season, whereas there was a pattern of fluctuation within three hours during the flood season. Under the baseline scenario, the marginal probabilities associated with the acute Cr^{6+} concentration declined from 0.8645 to 0.7657 throughout the dry season. Conversely, during the same period under the accident scenario, these probabilities experienced fluctuations ranging from 0.8649 to 0.9976. During the flood season, similar trends were observed, and the marginal probabilities related to the acute Cr^{6+} concentration decreased from 0.3691 to 0.3221 under the baseline scenario, while they fluctuated between 0.6349 and 0.8523 under the accident scenario.

Table 3
Water discharge, acute Cr^{6+} exposure and joint probability results for N3.

Period	Scenario	Time	Q (m^3/s)	Marginal Probability	Acute Cr^{6+} Concentration (mg/L)	Marginal Probability	Joint Probability
Dry Season	**Baseline**	2018/2/11 16:30	3.21385	0.4770	0.004277	0.8645	0.4327
	Scenario	2018/2/11 17:30	3.09873	0.4339	0.004276	0.8333	0.3850
		2018/2/11 18:30	3.08815	0.4310	0.004273	0.7975	0.3710
		2018/2/11 19:30	2.78522	0.3578	0.004269	0.7657	0.3019
	Accident	2018/2/11 16:30	3.21385	0.4770	0.010479	0.9966	0.4460
	Scenario	2018/2/11 17:30	3.09873	0.4339	0.018765	0.8649	0.3947
		2018/2/11 18:30	3.08815	0.4310	0.018028	0.9044	0.4041
		2018/2/11 19:30	2.78522	0.3578	0.01274	0.9976	0.3573
Flood Season	**Baseline**	2018/6/11 13:00	7.04179	0.6376	0.00721808	0.3691	0.0895
	Scenario	2018/6/11 14:00	7.66503	0.8523	0.00721579	0.3638	0.2319
		2018/6/11 15:00	7.02252	0.6282	0.00719816	0.3221	0.0632
	Accident	2018/6/11 13:00	7.04179	0.6376	0.01109268	0.9973	0.6349
	Scenario	2018/6/11 14:00	7.66503	0.8523	0.01695524	0.9980	0.8523
		2018/6/11 15:00	7.02252	0.6282	0.01231104	0.9987	0.8503

Copula functions were then constructed for each scenario and the best-fit Copula functions were selected based on D^2, shown in Fig. 5 and Table 4. D^2 of the binary Frank Copula was the smallest, with 0.0272 (baseline), 0.0267 (accident), 0.3610 (baseline), and 0.3801 (accident) during the dry and flood periods. Therefore, the Binary Frank Copula Function fit the simulation data best and was selected for the joint water quantity-quality probability function shown in Eqs. 18–21.

$$C_{b-d}(Q,\ Cr(VI)) = -\frac{1}{1.448}\ln\left[1+\frac{(e^{-1.448Q}-1)(e^{-1.448Cr(VI)}-1)}{e^{-1.448}-1}\right] \quad (18)$$

$$C_{b-a}(Q,\ Cr(VI)) = -\frac{1}{1.429}\ln\left[1+\frac{(e^{-1.429Q}-1)(e^{-1.429Cr(VI)}-1)}{e^{-1.429}-1}\right] \quad (19)$$

$$C_{f-d}(Q,\ Cr(VI)) = \frac{1}{7.644}\ln\left[1+\frac{(e^{7.644Q}-1)(e^{7.644Cr(VI)}-1)}{e^{7.644}-1}\right] \quad (20)$$

$$C_{f-a}(Q,\ Cr(VI)) = \frac{1}{7.472}\ln\left[1+\frac{(e^{7.472Q}-1)(e^{7.472Cr(VI)}-1)}{e^{7.472}-1}\right] \quad (21)$$

Based on the Copula functions, the joint water quantity–quality probability distribution was calculated and is shown in Table 4. During the dry period, after 16.5 h of exposure, the joint probability distribution reached its highest value of 0.4460 (higher than under the baseline scenario, i.e., 0.4327). Subsequently, the joint probability exhibited variability over the course of the 4-hour pollution scenario, fluctuating between 0.4460, 0.3947, 0.4041 and 0.3710. However, during the flood season, after 14 hours of exposure, the joint probability distribution attained its maximum value of 0.8523 (higher than under the baseline scenario, i.e., 0.4327). The joint probability then began to decrease from 0.8523 to 0.8503. In general, the joint probability distributions were higher under the accident scenario and lower for the baseline scenario during the flood period compared with the dry period.

3.3. Spatiotemporal exposure distribution map

Fig. 6 shows the spatiotemporal distribution map of acute exposure to drinking water sources in Nanjing City within the Yangtze River downstream watershed in China. As for risk sources (29 in total), five (N1–N5) would have an effect on drinking water sources when accidental heavy metal pollution occurred. There were two water sources (W3–W4, i.e., the Jiajiang Drinking Water Source Protection Zone and the Jiangpu-Pukou Drinking Water Source Protection Zone) with high exposures (AEI=1). Thereinto, W3 was highly susceptible to accidental heavy metal pollution caused by N1–N2 while W4 was influenced by N3–N4 during both the dry and flood seasons. Water source W5 (the Longtan Drinking Water Source Protection Zone) with medium exposure (AEI=0.5) was influenced by N23 during both the dry and flood seasons. The low exposure (AEI=0.25) water sources were W2 and W6 (i.e., the Baguazhou-Left Drinking Water Source Protection Zone and the Yanziji Drinking Water Source Protection Zone), and they were affected by N3 and N4 only during the flood season, respectively. Moreover, there remained two sources with zero exposure, including W1 and W7 (i.e., the Baguazhou-Main Drinking Water Source Protection Zone and the Zihuizhou Water Source Protection Zone).

4. Discussion

This study introduced a novel Copula-based spatiotemporal probabilistic model designed to precisely evaluate the interlinkages between water quantity and quality parameters to produce a robust framework for comprehensive analysis of hydrological systems. Consequently, an exposure distribution map for drinking water sources was produced that enabled the explicit identification and targeted management of critical risk sources, as well as the optimization of the selection of drinking water sources.

The data presented in Table 4 and Fig. 5 clearly demonstrated a strong negative correlation between water quantity and quality. During the dry season, when water discharge diminishes compared with the flood season, the spread of contaminants slowed, leading to a comparatively higher maximum concentration of the acute Cr^{6+} ion (i.e., 0.01877 mg/L during the flood season while 0.01696 mg/L during the dry season). This observation highlights the significance of discharge rates in influencing the dispersion and concentration of pollutants in aquatic environments. From a watershed management perspective, Fig. 6 underscores the critical importance of prioritizing the principal sources of risk for effective mitigation strategies. These sources are labeled N1 through N5, and are located in the downstream area of the Yangtze River near Nanjing City. Local stakeholders must intensify their focus on the electroplating plants in question, recognizing the imperative to enact rigorous water management practices. This includes imposing stringent controls over both the volume and quality of water in regions where drinking water sources, specifically identified as W3 and W4 (AEI=1), face substantial risks of contamination post-incident. Such proactive measures are vital to safeguard these sensitive areas from potential pollution and uphold the integrity of local water resources. Therefore, the proposed Copula-based spatiotemporal probabilistic model is a valuable benchmark for managing accidental risks and protecting drinking water sources effectively. In addition, it can establish a basis for judicious water allocation and management in the Yangtze River watershed of the future.

Integrating Copula functions into conventional simulation techniques enhances the exploration of the underlying mechanisms that govern both water discharge patterns and contaminant pollution in drinking water sources, and it provides several methodological advantages. To our knowledge, the foremost advantage lies in the ability to

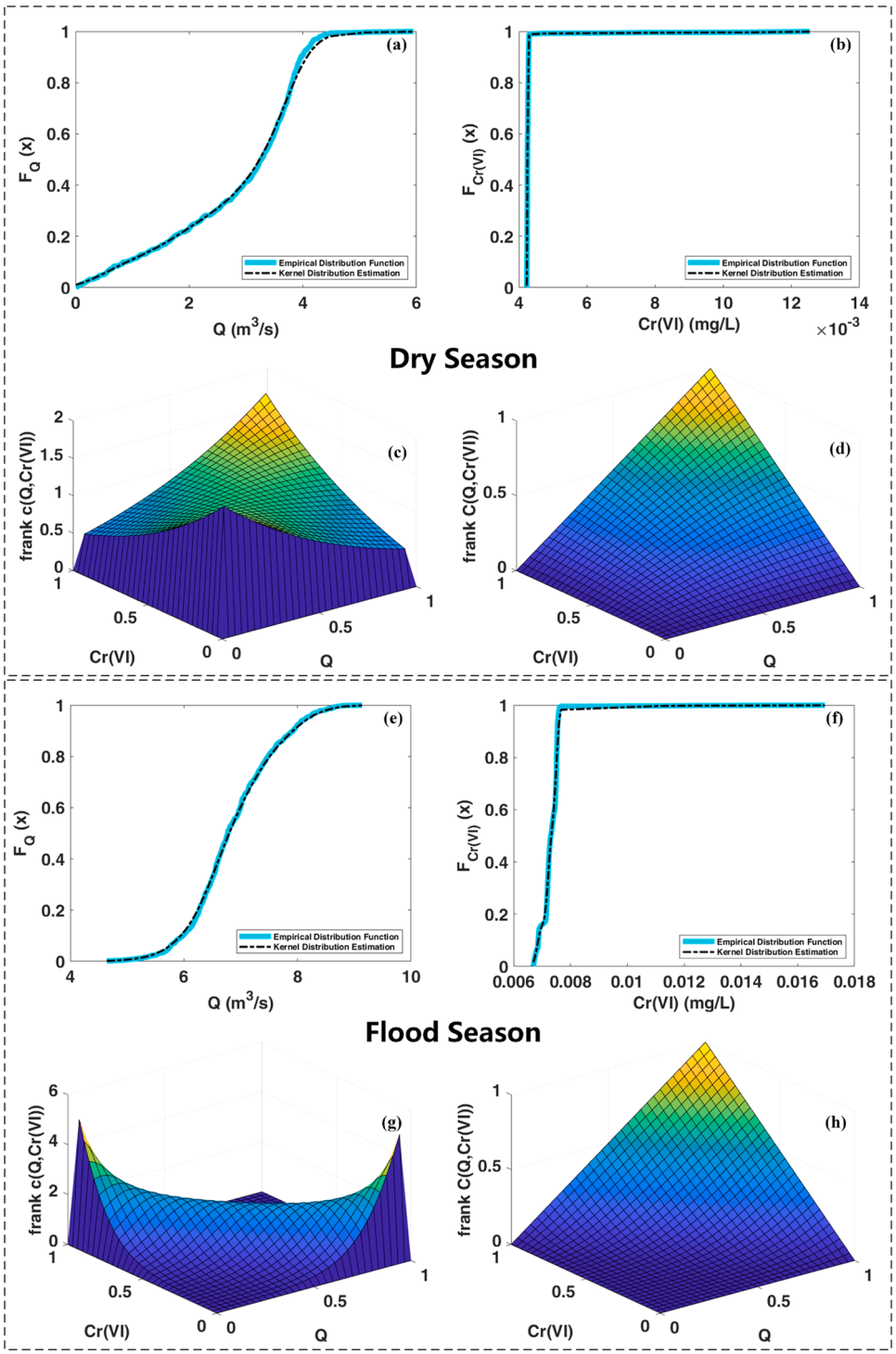

Fig. 5. Marginal probability distributions (a–b; e–f) and joint probability distributions (c–d; g–h) under the accident scenario during the dry and flood seasons.

meticulously construct a joint probability distribution model that accurately captures the relationships—be they nonlinear or asymmetric—between two quintessential variables: water quantity and quality in drinking water sources. Simultaneously, the Copula function maintains the integrity of all data related to water quantity and quality, ensuring no loss or distortion of information during the modeling process (Zentner, 2017; Zang et al., 2022). Hence, Copula analysis enables the generation of exact estimates and authentic simulations of the composite distribution that encompasses both water discharge and contaminant pollution across a full range of water pollution incidents, compared with impact risk methods (Zhou et al., 2021) or the hydrodamic and quality models (Wang et al., 2019) of the Yangtze River in Nanjing City. For example, when the highest heavy metal emergency occurred in the simulation during the flood season at a certain drinking water source (see Table 3 and Fig. 5), the joint probability was found to be 0.8523 based on the marginal probability of water quantity (0.8523) and quality (0.9980). This result was different from those of hydrodynamic models (Mbuh et al., 2019; Gomes et al., 2023) or multi-index methods (Dippong et al., 2018; Dippong and Resz, 2024 b), which treat water quantity and quality as two distinct causal factors, and

Table 4
The best-fit Copula function expressions and D^2 for N3.

Period	Scenario	Copula Functions	D^2
Dry Season	Baseline Scenario	$C(Q,\ Cr(VI)) = \int_{-}^{\varphi^{-1}(Q)} \int_{-}^{\varphi^{-1}(Cr(VI))} \frac{1}{2\pi\sqrt{1-(0.2139)^2}} \exp\left[\frac{-(s^2+t^2-2*(0.2139)st)}{2(1-(0.2139)^2)}\right] dsdt$	0.0342
		$C(Q,\ Cr(VI)) = (Q^{-0.0028} + Cr(VI)^{-0.0028} - 1)^{-\frac{1}{0.0028}}$	0.0297
		$C(Q,\ Cr(VI)) = \exp\left\{-\left[(-\ln Q)^{1.169} + (-\ln Cr(VI))^{1.169}\right]^{\frac{1}{1.169}}\right\}$	0.0807
		$C(Q,\ Cr(VI)) = -\frac{1}{1.448}\ln\left[1+\frac{(e^{-1.448Q}-1)(e^{-1.448Cr(VI)}-1)}{e^{-1.448}-1}\right]$	0.0272
	Accident Scenario	$C(Q,\ Cr(VI)) = \int_{-}^{\varphi^{-1}(Q)} \int_{-}^{\varphi^{-1}(Cr(VI))} \frac{1}{2\pi\sqrt{1-(0.2073)^2}} \exp\left[\frac{-(s^2+t^2-2*(-0.2073)st)}{2*(1-(-0.2073)^2)}\right] dsdt$	0.0369
		$C(Q,\ Cr(VI)) = (Q^{-0.003} + Cr(VI)^{-0.003} - 1)^{-\frac{1}{0.003}}$	0.0786
		$C(Q,\ Cr(VI)) = \exp\left\{-\left[(-\ln Q)^{1.1562} + (-\ln Cr(VI))^{1.1562}\right]^{\frac{1}{1.1562}}\right\}$	0.0368
		$C(Q,\ Cr(VI)) = -\frac{1}{1.429}\ln\left[1+\frac{(e^{-1.429Q}-1)(e^{-1.429Cr(VI)}-1)}{e^{-1.429}-1}\right]$	0.0267
Flood Season	Baseline Scenario	$C(Q,\ Cr(VI)) = \int_{-}^{\varphi^{-1}(Q)} \int_{-}^{\varphi^{-1}(Cr(VI))} \frac{1}{2\pi\sqrt{1-(-0.7534)^2}} \exp\left[\frac{-(s^2+t^2-2*(-0.7534)st)}{2(1-(-0.7534)^2)}\right] dsdt$	0.3719
		$C(Q,\ Cr(VI)) = (Q^{-0.0017} + Cr(VI)^{-0.0017} - 1)^{-\frac{1}{0.0017}}$	0.6324
		$C(Q,\ Cr(VI)) = \exp\left\{-\left[(-\ln Q)^{1.03} + (-\ln Cr(VI))^{1.03}\right]^{\frac{1}{1.03}}\right\}$	0.8435
		$C(Q,\ Cr(VI)) = \frac{1}{7.644}\ln\left[1+\frac{(e^{7.644Q}-1)(e^{7.644Cr(VI)}-1)}{e^{7.644}-1}\right]$	0.3610
	Accident Scenario	$C(Q,\ Cr(VI)) = \int_{-}^{\varphi^{-1}(Q)} \int_{-}^{\varphi^{-1}(Cr(VI))} \frac{1}{2\pi\sqrt{1-(-0.7281)^2}} \exp\left[\frac{-(s^2+t^2-2*(-0.7281)st)}{2(1-(-0.7281)^2)}\right] dsdt$	0.4128
		$C(Q,\ Cr(VI)) = (Q^{-0.0014} + Cr(VI)^{-0.0014} - 1)^{-\frac{1}{0.0014}}$	0.8167
		$C(Q,\ Cr(VI)) = \exp\left\{-\left[(-\ln Q)^{1.13} + (-\ln Cr(VI))^{1.13}\right]^{\frac{1}{1.13}}\right\}$	0.9435
		$C(Q,\ Cr(VI)) = \frac{1}{7.472}\ln\left[1+\frac{(e^{7.472Q}-1)(e^{7.472Cr(VI)}-1)}{e^{7.472}-1}\right]$	0.3801

multi-index methods that view them as isolated independent elements, Copula functions uniquely trace the intricate relationships between these variables, offering a comprehensive approach to water environment assessments. Another advantage is that uncertainty can be contained in the Copula models in the form of a probability distribution due to high uncertainty during water pollution emergencies (Paredes-Arquiola et al., 2010; Tscheikner-Gratl et al., 2019; Liu et al., 2021). The probability distribution is relatively more credible compared to the traditional numerical simulation (Hur et al., 2018; Shin, 2023). In addition, the construction of Copula functions requires a smaller number of data parameters, rendering them more versatile than hydrodynamic approaches (Cai et al., 2019; Yue et al., 2022).

However, further enhancements can be implemented to this spatiotemporal probabilistic model based on Copula analysis. First, the acquisition of real-time data for water pollution emergencies presents significant challenges, and this subsequently complicates the processes of calibration and validation of the collected data. Future investigations should explore indoor simulation experiments to provide additional support for the predictive reliability. Second, in this study, our analysis focused solely on two variables: the discharge rate and acute chromium (Cr^{6+}) exposure, for calculating the impact of accidental water pollution. In practice, it would be prudent to incorporate a broader range of indicators into the modeling process, including ecological, meteorological, and various environmental contaminant factors, to reflect more accurately the complexity of real-world aquatic environments. In addition, the integration of additional potential Copula functions within multivariable joint probability distribution models is worth exploration to produce an optimized analytical framework (Zang et al., 2022).

5. Conclusions

This research presented a Copula-based spatiotemporal probabilistic model to quantitatively address the internal correlation between water quantity and quality for drinking water sources. Copula functions are especially suitable to explore relationships between variables as they can separate the dependence structures from the variables' marginal distributions. Compared with hydrodynamic models or multi-index methods, Copula theory can better characterize joint probability distributions with a high degree of accuracy. In the case study of the Yangtze River downstream watershed in Nanjing, 29 electroplating plants were chosen to quantitatively estimate the joint effects between water discharge and contaminant pollution on seven drinking water sources. The results indicated a strong negative correlation between water quantity and quality. The spatiotemporal exposure distribution map showed that five risk sources (N1–N5) were key sources, while two drinking water sources (W3–W4; AEI=1) would be easily affected and require more attention. Although this study successfully demonstrated the feasibility of quantifying the complex interrelationships between water quality and quantity, the next step is the incorporation of more environmental contaminant factors and more contaminant pollutants into the model. In summary, this research enhances our understanding of the joint behavior of multiple variables affecting drinking water sources in the event of accidents.

CRediT authorship contribution statement

Kun Zhang: Writing – review & editing. **Yingying Zhu:** Software. **Jinwei Bian:** Methodology. **Saige Wang:** Writing – review & editing. **Yushun Qi:** Software. **Naifeng Lin:** Writing – review & editing.

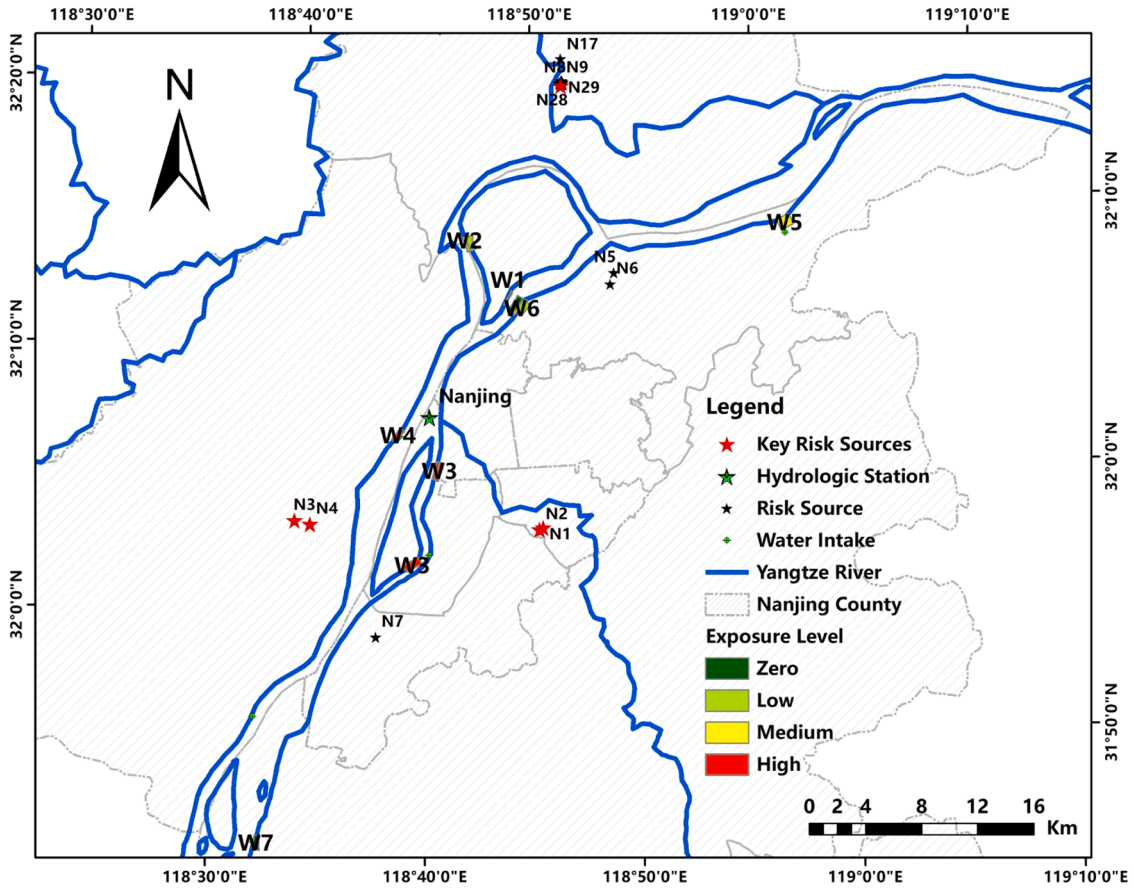

Fig. 6. Spatiotemporal exposure distribution map for drinking water sources in the downstream watershed of the Yangtze River in Nanjing, China.

Xiaojuan Xu: Writing – original draft, Software, Conceptualization. **Jing Liu:** Writing – original draft, Software, Project administration, Methodology, Funding acquisition, Conceptualization. **Renzhi Liu:** Validation, Resources. **Changxin Zou:** Supervision, Resources.

Declaration of Competing Interest

The authors declare that they have no known competing financial interests or personal relationships that could have appeared to influence the work reported in this paper.

Data Availability

Data will be made available on request.

Acknowledgements

This research was supported by the Youth Foundation in the Jiangsu Province of China (No. BK20220205), the National Natural Science Foundation of China Youth Science Program (No. 72103022) and the Youth Foundation in the Nanjing Institute of Environmental Sciences of China (No. GYZX230309). The authors are grateful to the Department of Ecology and Environment of Nanjing in Jiangsu Province.

References

Ali, M.M., Islam, M.S., Islam, A.R.M.T., Bhuyan, M.S., Ahmed, A.S.S., Rahman, M.Z., Rahman, M.M., 2022. Toxic metal pollution and ecological risk assessment in water and sediment at ship breaking sites in the Bay of Bengal Coast, Bangladesh. Mar. Pollut. Bull. 175, 113274.

Cai, J.Y., Wang, X., Cai, Y.P., Wei, C.X., Liao, Z.M., Liu, D., Li, C.H., Liu, Q., 2023. An integrated connectivity diagnostics and dependency analysis framework for supporting water replenishment management. J. Hydrol. 620, 129442.

Cai, Y.P., Cai, J.Y., Xu, L.Y., Tan, Q., Xu, Q., 2019. Integrated risk analysis of water-energy nexus systems based on systems dynamics, orthogonal design and copula analysis. Renew. Sust. Energy Rev. 99, 125–137.

Campanho, L.M.B., Picharillo, C., Ranieri, V.E.L., Okawa, C.M.P., 2021. Socioeconomic and environmental impacts of water markets: a literature review. Desenvolv. e Meio Ambient. 56.

Cao, X., Mukandinda Cyuzuzo, C., Saiken, A., Song, B., 2021. A linear additivity water resources assessment indicator by combining water quantity and water quality. Ecol. Indic. 121, 106990.

Chen, L., Li, J., Xu, J., Liu, G., Wang, W., Jiang, J., Shen, Z., 2022. New framework for nonpoint source pollution management based on downscaling priority management areas. J. Hydrol. 606, 127433.

Chen, T., Wang, Y., Gardner, C., Wu, F., 2020. Threats and protection policies of the aquatic biodiversity in the Yangtze River. J. Nat. Conserv. 58, 125931.

DHI, 2017a. MIKE 21 Flow Model & MIKE 21 Flood Screening Tool Hydrodynamic Module. Scientific Documentation. Danish Hydraulic Institute, Denmark.

DHI, 2017b. Heavy Metal: MIKE ECO Lab Template. Scientific Description. Danish Hydraulic Institute, Denmark.

Di Toro, D.M., Mahony, J.D., Kirchgraber, P.R., O'Byrne, A.L., Pasquale, L.R., Piccirilli, D.C., 1986. Effects of nonreversibility, particle concentration, and ionic strength on heavy-metal sorption. Environ. Sci. Technol. 20, 55–61.

Dippong, T., Resz, M.A., 2022. Quality and health risk assessment of groundwaters in the protected area of Tisa river basin. Int. J. Environ. Res. Public Health 19 (22), 14898.

Dippong, T., Resz, M.A., 2024 a. . Heavy metal contamination assessment and potential human health risk of water quality of lakes situated in the protected area of Tisa, Romania. Heliyon 10 (7).

Dippong, T., Resz, M.A., 2024 b. . Chemical assessment of drinking water quality and associated human health risk of heavy metals in Gutai Mountains, Romania. Toxics 12 (3), 168.

Dippong, T., Mihali, C., Năsui, D., Berinde, Z., Butean, C., 2018. Assessment of water physicochemical parameters in the Strîmtori-Firiza Reservoir in Northwest Romania. Water Environ. Res. 90 (3), 220–233.

Dippong, T., Hoaghia, M.A., Senila, M., 2022. Appraisal of heavy metal pollution in alluvial aquifers. Study case on the protected area of Ronișoara Forest, Romania. Ecol. Indic. 143, 109347.

Dippong, T., Mihali, C., Avram, A., 2023. Water physico-chemical indicators and metal assessment of teceu lake and the adjacent groundwater located in a natura 2000 protected area, NW of Romania. Water 15 (22), 3996.

Dong, W., Zhang, Y., Zhang, L., Ma, W., Luo, L., 2023. What will the water quality of the Yangtze River be in the future? Sci. Total Environ. 857, 159714.

Frees, E.W., Valdez, E.A., 1998. Understanding relationships using copulas. N. Am. Actuar. J. 2, 1–25.
Goka, E., Beaurepaire, P., Homri, L., Dantan, J.-Y., 2019. Probabilistic-based approach using Kernel Density Estimation for gap modeling in a statistical tolerance analysis. Mech. Mach. Theory 139, 294–309.
Gomes, M.N., do Lago, C.A.F., Rápalo, L.M.C., Oliveira, P.T.S., Giacomoni, M.H., Mendiondo, E.M., 2023. HydroPol2D — Distributed hydrodynamic and water quality model: Challenges and opportunities in poorly-gauged catchments. J. Hydrol. 625, 129982.
He, M., Liu, G., Li, Y., Zhou, L., Arif, M., Liu, Y., 2023. Spatial-temporal distribution, source identification, risk assessment and water quality assessment of trace elements in the surface water of typical tributary in Yangtze River delta, China. Mar. Pollut. Bull. 192, 115035.
Honeyman, B.D., Santschi, P.H., 1988. Metals in aquatic systems. Environ. Sci. Technol. 22, 862–871.
Huang, Y., Cai, Y., Dai, C., He, Y., Wan, H., Guo, H., Zhang, P., 2024. An integrated simulation-optimization approach for combined allocation of water quantity and quality under multiple uncertainties. J. Environ. Manag. 363, 121309.
Hur, S., Nam, K., Kim, J., Kwak, C., 2018. Development of urban runoff model FFC-QUAL for first-flush water-quality analysis in urban drainage basins. J. Environ. Manag. 205, 73–84.
Issakhov, A., Alimbek, A., Zhandaulet, Y., 2021. The assessment of water pollution by chemical reaction products from the activities of industrial facilities: numerical study. J. Clean. Prod. 282, 125239.
Jiang, W., Pokharel, B., Lin, L., Cao, H., Carroll, K.C., Zhang, Y., Galdeano, C., Musale, D. A., Ghurye, G.L., Xu, P., 2021. Analysis and prediction of produced water quantity and quality in the Permian Basin using machine learning techniques. Sci. Total Environ. 801, 149693.
Jiangsu Province Water Resources Bulletin (JPWRB), 2021. Jiangsu: China Statistical Publishing House.
Jin, Y., Jiang, Y.H., Zhou, Q.P., Wang, X.L., Zhang, H., Mei, S.J., Chen, Z., Yang, H., Lv, J. S., Hou, L.L., Qi, Q.J., Jia, Z.Y., Yang, H., 2023. Characteristics of heavy metals in mainstream sediment of the Yangtze River downstream and its ecological risk assessment. Geol. China 1–20.
Khan, F.I., 2001. Use maximum-credible accident scenarios for realistic and reliable risk assessment. Chem. Eng. Prog. 97, 56–65.
Li, J., Shen, Z., Cai, J., Liu, G., Chen, L., 2023. Copula-based analysis of socio-economic impact on water quantity and quality: a case study of Yitong River, China. Sci. Total Environ. 859, 160176.
Liao, R., Jin, Z., Chen, M., Li, S., 2020. An integrated approach for enhancing the overall performance of constructed wetlands in urban areas. Water Res 187, 116443.
Liu, J., Liu, R., Zhang, Z., Zhang, H., Cai, Y., Yang, Z., Kuikka, S., 2021b. Copula-based exposure risk dynamic simulation of dual heavy metal mixed pollution accidents at the watershed scale. J. Environ. Manag. 277, 111481.
Liu, J., Liu, R., Yang, Z., Kuikka, S., 2021a. Quantifying and predicting ecological and human health risks for binary heavy metal pollution accidents at the watershed scale using Bayesian Networks. Environ. Pollut. 269, 116125.
Liu, W., Wang, D., Singh, V.P., Wang, Y., Zeng, X., Ni, L., Tao, Y., Wu, J., Liu, J., Zou, Y., He, R., Zhang, J., 2020. A hybrid statistical model for ecological risk integral assessment of PAHs in sediments. J. Hydrol. 583, 124612.
Liu, Y., Cao, S., Zhang, X., Li, F., Li, X., 2018. Joint improvement of river water quality indicators based on a multivariate joint probability distribution of the discharge and water quality. Hydrol. Res. 49, 1915–1928.
Liu, Y., Wang, J., Cao, S., Han, B., Liu, S., Chen, D., 2022. Copula-based framework for integrated evaluation of water quality and quantity: a case study of Yihe River, China. Sci. Total Environ. 804, 150075.
Liu, Z., Sang, J., Zhu, M., Feng, R., Ding, X., 2024. Prediction and countermeasures of heavy metal copper pollution accident in the Three Gorges Reservoir Area. J. Hazard Mater. 465, 133208.
Manyepa, P., Gani, K.M., Seyam, M., Banoo, I., Genthe, B., Kumari, S., Bux, F., 2024. Removal and risk assessment of emerging contaminants and heavy metals in a wastewater reuse process producing drinkable water for human consumption. Chemosphere 361, 142396.
Manzar, M.S., Benaafi, M., Costache, R., Alagha, O., Mu'azu, N.D., Zubair, M., Abdullahi, J., Abba, S.I., 2022. New generation neurocomputing learning coupled with a hybrid neuro-fuzzy model for quantifying water quality index variable: a case study from Saudi Arabia. Ecol. Inform. 70, 101696.
Mbuh, M.J., Mbih, R., Wendi, C., 2019. Water quality modeling and sensitivity analysis using Water Quality Analysis Simulation Program (WASP) in the Shenandoah River watershed. Phys. Geogr. 40, 127–148.
McManamay, R.A., 2014. Quantifying and generalizing hydrologic responses to dam regulation using a statistical modeling approach. J. Hydrol. 519, 1278–1296.
Meng, F., Cao, R., Zhu, X., Zhang, Y., Liu, M., Wang, J., Chen, J., Geng, N., 2024. A nationwide investigation on the characteristics and health risk of trace elements in surface water across China. Water Res 250, 121076.
Ministry of Water Resources, P. R. China (MWR), 2019. In: Annual Hydrological Report, P. R. China, vol. 7. Main Stream of Changjiang River, Beijing China. Hydrological Data of Changjiang River Basin. No. 7.
Müller, B., Berg, M., Yao, Z., Zhang, X., Wang, D., Pfluger, A., 2008. How polluted is the Yangtze River? Water quality downstream from the Three Gorges Dam. Sci. Total Environ. 402, 232–247.
Najafzadeh, M., Ahmadi-Rad, E.S., Gebler, D., 2024. Ecological states of watercourses regarding water quality parameters and hydromorphological parameters: deriving empirical equations by machine learning models. Stoch. Environ. Res. Risk A. 38, 665–688.
Nyjfeler, U.P., Santschi, P.H., Li, Y.H., 1986. The relevance of scavenging kinetics to modeling of sediment-water interactions in natural waters. Limnol. Oceano 31, 277–292.
Paredes-Arquiola, J., Andreu-Álvarez, J., Martín-Monerris, M., Solera, A., 2010. Water quantity and quality models applied to the Jucar River Basin, Spain. Water Resour. Manag. 24, 2759–2779.
Park, D., Markus, M., Jung, K., Um, M.-J., 2019. Uncertainty analysis of the relationship between discharge and nitrate concentration in the Lower Illinois River using a copula model. J. Clean. Prod. 222, 310–323.
Schleich, B., Wartzack, S., 2018. Gap hull estimation for rigid mechanical joints considering form deviations and multiple pairs of mating surfaces. Mech. Mach. Theory 128, 444–460.
Seo, J., Won, J., Lee, H., Kim, S., 2024. Probabilistic monitoring of meteorological drought impacts on water quality of major rivers in South Korea using copula models. Water Res. 251, 121175.
Shi, W., Wang, W., Yu, S., Liang, L., Zhong, J., Yi, Y., Li, S.-L., 2024. Influences of hydrodynamics on dissolved inorganic carbon in deep subtropical reservoir: insights from hydrodynamic model and carbon isotope analysis. Water Res. 250, 21058.
Shin, S., Her, Y., Muñoz-Carpena, R., Yu, X., Martinez, C., Singh, A., 2023. Climate change impacts on water quantity and quality of a watershed-lake system using a spatially integrated modeling framework in the Kissimmee River – Lake Okeechobee system. J. Hydrol. -Reg. Stud. 47, 101408.
Shokri, A., Bozorg Haddad, O., Mariño, M.A., 2014. Multi-objective quantity–quality reservoir operation in sudden pollution. Water Resour. Manag. 28, 567–586.
Sklar, A., 1959. Fonctions de répartition `a n dimensions et leurs marges, vol. 8. Publ Inst Stat Univ Paris, pp. 229–231, 229–231.
Tai, V.C., Uhlen, K., 2015. Resampling of data for offshore grid design based on kernel density estimation and genetic algorithm. Energy Procedia 80, 365–375.
Tscheikner-Gratl, F., Bellos, V., Schellart, A., Moreno-Rodenas, A., Muthusamy, M., Langeveld, J., Clemens, F., Benedetti, L., Rico-Ramirez, M.A., de Carvalho, R.F., Breuer, L., Shucksmith, J., Heuvelink, G.B.M., Tait, S., 2019. Recent insights on uncertainties present in integrated catchment water quality modelling. Water Res. 150, 368–379.
Varol, M., Tokatli, C., 2022. Seasonal variations of toxic metal(loid)s in groundwater collected from an intensive agricultural area in northwestern Turkey and associated health risk assessment. Environ. Res 204, 111922.
Varol, M., Tokatli, C., 2023. Evaluation of the water quality of a highly polluted stream with water quality indices and health risk assessment methods. Chemosphere 311, 137096.
Wang, G., Qiu, G., Wei, J., Guo, Z., Wang, W., Liu, X., Song, Y., 2023. Activated carbon enhanced traditional activated sludge process for chemical explosion accident wastewater treatment. Environ. Res. 225, 115595.
Wang, P., Lu, X., Jin, W., Chen, M., Ma, Y., Xiong, P., 2024. Quantifying pollution contributions across a reticular river network: insights from water quantity composition analysis. Ecol. Indic. 166, 112269.
Wang, Q.Q., Wu, H., Wang, L.C., Ji, X.M., 2019. Study on the impact of sudden pollution on water sources: a case study of Nanjing section of Yangtze River. J. Ecol. Rural Environ. 35 (12), 1557–1563.
Wang, W.C., Xu, D.M., Chau, K.W., 2014. Assessment of river water quality based on theory of variable fuzzy sets and fuzzy binary comparison method. Water Resour. Manag. 28, 4183–4200.
Wang, X., Zang, N., Liang, P., Cai, Y., Li, C., Yang, Z., 2017. Identifying priority management intervals of discharge and TN/TP concentration with copula analysis for Miyun Reservoir inflows, North China. Sci. Total Environ. 609, 1258–1269.
Warren, I.R., Bach, H.K., 1992. MIKE 21: a modelling system for estuaries, coastal waters and seas. Environ. Modell. Softw. 7, 229–240.
Xie, H., Yang, X., Xu, J., Zhong, D., 2023. Heavy metals pollution and potential ecological health risk assessment in the Yangtze River reaches. J. Environ. Chem. Eng. 11, 109489.
Xu, J., Xu, M., Zhao, Y., Wang, S., Tao, M., Wang, Y., 2021. Spatial-temporal distribution and evolutionary characteristics of water environment sudden pollution incidents in China from 2006 to 2018. Sci. Total Environ. 801, 149677.
Xue, B., Zhang, H., Wang, Y., Tan, Z., Zhu, Y., Shrestha, S., 2021. Modeling water quantity and quality for a typical agricultural plain basin of northern China by a coupled model. Sci. Total Environ. 790, 148139.
Yang, H., Wang, J., Li, J., Zhou, H., Liu, Z., 2021. Modelling impacts of water diversion on water quality in an urban artificial lake. Environ. Pollut. 276, 116694.
Yu, R., Zhang, C., 2021. Early warning of water quality degradation: a copula-based Bayesian network model for highly efficient water quality risk assessment. J. Environ. Manag. 292, 112749.
Yu, S., He, L., Lu, H., 2016. An environmental fairness based optimisation model for the decision-support of joint control over the water quantity and quality of a river basin. J. Hydrol. 535, 366–376.
Yue, W., Yu, S., Xu, M., Rong, Q., Xu, C., Su, M., 2022. A Copula-based interval linear programming model for water resources allocation under uncertainty. J. Environ. Manag. 317, 115318.
Zang, N., Zhu, J., Wang, X., Liao, Y., Cao, G., Li, C., Liu, Q., Yang, Z., 2022. Eutrophication risk assessment considering joint effects of water quality and water quantity for a receiving reservoir in the South-to-North Water Transfer Project, China. J. Clean. Prod. 331, 129966.
Zavareh, M.M.J., Mahjouri, N., Rahimzadegan, M., Rahimpour, M., 2023. A drought index based on groundwater quantity and quality: application of multivariate copula analysis. J. Clean. Prod. 417, 137959.
Zentner, I., 2017. A general framework for the estimation of analytical fragility functions based on multivariate probability distributions. Struct. Saf. 64, 54–61.

Zhai, A., Hou, B., Ding, X., Huang, G., 2021. Hazardous chemical accident prediction for drinking water sources in Three Gorges Reservoir. J. Clean. Prod. 296, 126529.
Zhang, C., Nong, X., Behzadian, K., Campos, L.C., Chen, L., Shao, D., 2024. A new framework for water quality forecasting coupling causal inference, time-frequency analysis and uncertainty quantification. J. Environ. Manag. 350, 119613.
Zhang, S.Q., Li, Y.P., Huang, G.H., Ding, Y.K., Yang, X., 2023. Developing a copula-based input-output method for analyzing energy-water nexus of Tajikistan. Energy 266, 126511.
Zhang, X., Zhang, C., Song, C., Fan, L.M., Qiu, L.P., Meng, S.L., Chen, J.Z., 2017. Heavy metal content of water and risk assessment in the lower reaches of the Yangtze River. Chin. Agric. Sci. Bull. 33 (30), 67–73.
Zhao, J., Fang, G., Wang, X., Zhong, H., 2024. Joint optimization of urban water quantity and quality allocation in the plain river network area. Sustainability 16, 1368.
Zhou, Q., Zhang, J., Niu, Y., Wang, J., 2021. Environmental risk assessment and regulatory rating of water sources along the Yangtze River's Nanjing section under the influence of multiple risk sources. Sustainability 13 (3), 1484.